Photonic multi-shape UWB pulse generation using a semiconductor optical amplifier-based nonlinear optical loop mirror*

Luo Bo-Wen(罗博文), Dong Jian-Ji(董建绩)†, Yu Yuan(于 源), Yang Ting(杨 婷), and Zhang Xin-Liang(张新亮)

Wuhan National Laboratory for Optoelectronics, School of Optoelectronic Science and Engineering, Huazhong University of Science and Technology, Wuhan 430074, *China*

(Received 17 June 2012; revised manuscript received 2 August 2012)

We propose and demonstrate a scheme to implement photonic multi-shape ultra-wideband (UWB) signal generation using a semiconductor optical amplifier (SOA) based nonlinear optical loop mirror (NOLM). By employing the cross phase modulation (XPM) effect, cross gain modulation (XGM), or both, multi-shape UWB waveforms are generated including monocycle, doublet, triplet, and quadruplet pulses. Both the shapes and polarities of the generated pulses are flexible to adjust, which may be very useful in UWB pulse shape modulation and pulse polarity modulation.

Keywords: semiconductor optical amplifier, ultra-wideband generation, radio frequency photonics

PACS: 32.30.Bv, 84.40.–x, 42.79.Sz **DOI:** 10.1088/1674-1056/22/2/023201

1. Introduction

Ultra-wideband (UWB) technology has attracted significant interest as a promising solution in short-range high speed wireless communication and sensor networks due to its intrinsic advantages, such as low power consumption, immunity to multipath fading, high data-rate, low required signal-to-noise ratio, and huge bandwidth.[1–3] The United States' Federal Communications Commission (FCC) has allocated 7.5-GHz spectral band from 3.1 GHz to 10.6 GHz for unlicensed use. Based on the FCC definition, a UWB signal should have a spectral bandwidth that is greater than 500 MHz or a fraction bandwidth that is greater than 20%. However, UWB distribution is limited to only a few meters or tens of meters in free space due to its low power spectra density. UWB-over-fiber (UWBoF) is considered to be an effective technology to increase the coverage of UWB signals thanks to the low loss and broad bandwidth of optical fibers and UWB communication systems can be further integrated into optical networks. In the UWBoF system, it is desirable that the UWB pulse can be generated in the optical domain to avoid the extra cost of the hardware required for the electrical–optical conversion. Additionally, photonic generation of the UWB signal has some other features, such as small size, light weight, great tunability, and immunity to electromagnetic interference.[4] In recent years, several schemes have been reported that aim to generate the UWB signal in the optical domain, such as using cross phase modulation (XPM) assisted by a frequency shift optical bandpass filter (BPF),[5–8] using the cross gain modulation (XGM) effects and gain saturation effects in a semiconductor optical amplifier (SOA),[9–12] using a highly nonlinear fiber based loop mirror,[13,14] using cross polarization modulation,[15,16] using an optically injected chaotic semiconductor laser,[17] and using stimulated Brillouin scattering-amplified spontaneous emission.[18] Most of the reported methods could only generate one or two types of UWB signals. Reference [6] proposed a scheme to generate four types of UWB signal including monocycle, doublet, triplet, and quadruplet pulses. However, these four types of UWB signals are highly dependent on the shapes of the driving electrical signals. In other words, the input signal needs to change in the electrical domain.

In this paper, we propose a novel scheme for photonic generation of multiple types of UWB signals by using an SOA-based nonlinear optical loop mirror (NOLM). In our scheme, two probe lights are launched into the loop and one of them co-propagates with the pump light. These two probe lights interact with the pump light for the XPM effect. Then the phase shifts on the probe lights are converted to intensity modulation at the output port of the NOLM. Combining the pump light and the probe lights with proper weight and time delay, multiple shapes of UWB signals can be generated including monocycle, doublet, triplet, and quadruplet pulses. The shape of the generated pulses can be flexibly adjusted.

2. Operation principle

The operation principle of multi-shape UWB signal generation is shown in Fig. 1. A probe light (Probe 1) with a central wavelength of λ_1 is launched into the loop and divided into two parts, the clockwise (CW) light and the counter-clockwise (CCW) light, by a 50:50 optical coupler (OC1). Then these two parts are fed into the SOA with a relative delay ΔT which

*Project supported by the National Basic Research Program of China (Grant No. 2011CB301704), the National Natural Science Foundation for Distinguished Young Scholars (Grant No. 61125501), and the National Natural Science Foundation of China (Grant Nos. 60901006 and 11174096).

†Corresponding author. E-mail: jjdong@mail.hust.edu.cn

© 2013 Chinese Physical Society and IOP Publishing Ltd

can be adjusted by tuning the optical delay line (OTDL) in the loop. Both CW and CCW lights will be phase modulated by the pump light for the XPM effect in the SOA. In our system, a Gaussian pulse is used as the pump light. Then the introduced phase shift of probe signals is proportional to the power of the Gaussian pulse. Therefore the optical field of the CW light and the CCW light can be written as

$$E_{\mathrm{CW}}(t) = \frac{\sqrt{2}}{2} E_{\mathrm{in}}(t) \exp\{\mathrm{j}[\varphi(P_{\mathrm{pump}}(t))]\}, \tag{1}$$

$$E_{\mathrm{CCW}}(t-\Delta T) = \frac{\sqrt{2}}{2} E_{\mathrm{in}}(t-\Delta T) \times \exp\left\{\mathrm{j}\left[\varphi(P_{\mathrm{pump}}(t)) + \frac{\pi}{2}\right]\right\}, \tag{2}$$

where E_{in} is the initial optical field of the Probe 1, and P_{pump} is the power of the pump pulse and denotes the phase shift induced by the pump power. After propagation in the SOA, the CW light and the CCW light are combined at the OC1, and the output power of the NOLM reflection port (Port 1) can be written as

$$P_{\mathrm{reflection}}(t) = \frac{P_{\mathrm{in}}(t)}{2} \cdot \{1+\cos[\varphi(P_{\mathrm{pump}}(t)) - \varphi(P_{\mathrm{pump}}(t-\Delta T))]\}, \tag{3}$$

where P_{in} is the initial power of the Probe 1, which can be seen as a constant in the system. From Eq. (3), the phase shifts are converted to two intensity notches with a relative delay ΔT at Port 1 as shown in Fig. 2(a).

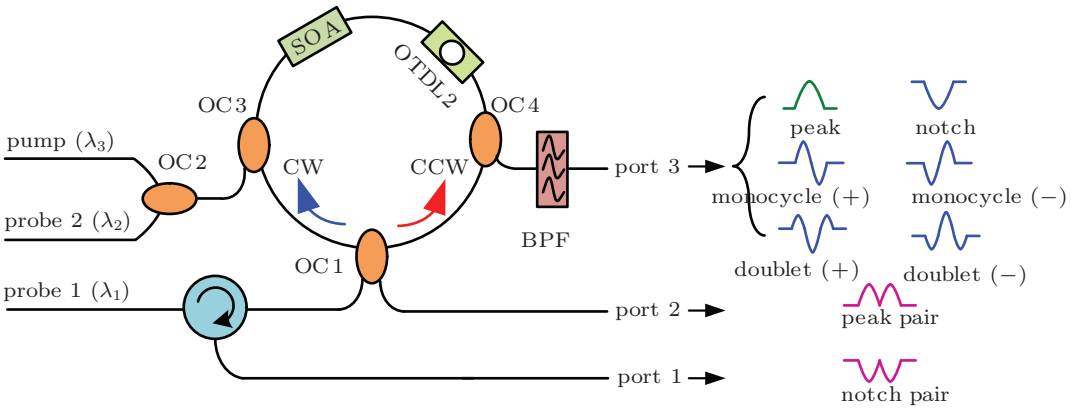


Fig. 1. (color online) Operation principle of multi-shape UWB signal generation, SOA: semiconductor optical amplifier, OTDL: optical tunable delay line, BPF: bandpass filter, OC: optical coupler.

Similarly, the intensity of the output of the pass port (Port 2) of the NOLM can be written as

$$P_{\mathrm{pass}}(t) = \frac{P_{\mathrm{in}}(t)}{2} \cdot \{1-\cos[\varphi(P_{\mathrm{pump}}(t)) - \varphi(P_{\mathrm{pump}}(t-\Delta T))]\}. \tag{4}$$

From Eq. (4), the phase shifts are converted to two intensity peaks with a relative delay ΔT at Port 2, as shown in Fig. 2(b). When these peak pair and notch pair are incoherent and combined with proper delay, a monocycle pair with reversed polarity can be generated as shown in Fig. 3(a).

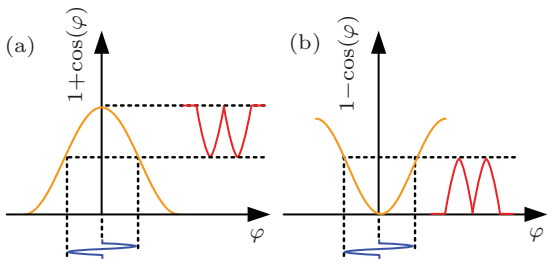


Fig. 2. (color online) Phase modulation to intensity modulation conversion at Port 1 (a), and Port 2 (b).

At the same time, another probe light (Probe 2) with a central wavelength of λ_2 co-propagates with the pump light into the SOA for both XGM and XPM simultaneously. A bandpass filter (BPF) is placed at the Port 3 as shown in Fig. 1. When the central wavelength of the BPF is set at λ_3, the pump light is filtered out and the output of Port 3 is an intensity peak, as shown in the dash-dotted line of Fig. 3(c). When the central wavelength of the BPF is set to be λ_2, the Probe 2 is filtered out and the output of Port 3 becomes an intensity notch for the XGM effect, as shown in the dashed line of Fig. 3(b). Moreover, by detuning the BPF properly, the phase shift of Probe 2 can be converted into a differential intensity signal due to the frequency discrimination of the BPF. Aligning the probe carrier at the linear slope or quadrature slope of the detuning BPF, one can obtain a monocycle pulse, shown as the dashed line of Figs. 3(d) and 3(e) or doublet pulse, shown as the dashed line of Figs. 3(f) and 3(g). The detailed operation principle can be found in Ref. [5].

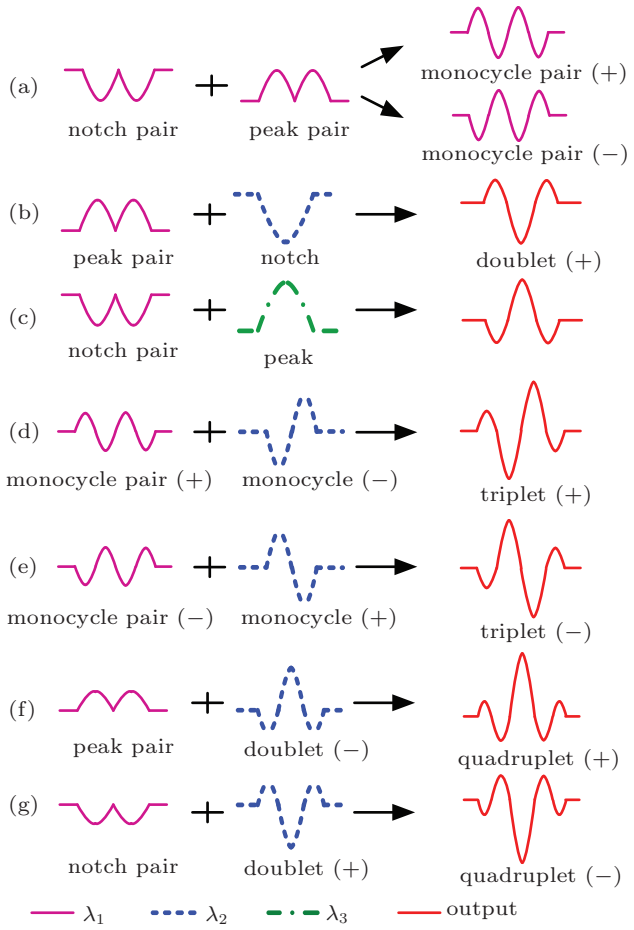


Fig. 3. (color online) Evolution of multi-shape UWB signal generation: (a) monocycle pair, (b) positive doublet, (c) negative doublet, (d) positive triplet, (e) negative triplet, (f) positive quadruplet, (g) negative quadruplet.

In the NOLM configuration, three output ports (Port 1, Port 2, and Port 3) have different temporal waveforms. If we carefully tune the central wavelength of the BPF and then incoherently combine these waveforms at different output ports with proper weight and proper time delay, we can obtain bipolar doublet, triplet, and quadruplet pulses. The evolutions of different UWB synthesis are shown in Figs. 3(b)–3(g).

3. Experimental demonstration and discussion

The experimental setup for photonic multi-shape UWB signal generation is shown in Fig. 4. Probe 1 with a central wavelength of 1549.2 nm and Probe 2 with a central wavelength of 1554.8 nm are emitted from two laser diodes (LD1 and LD2), respectively. The pump light with a central wavelength of 1561.4 nm is emitted from LD3 and modulated by a Mach–Zehnder modulator (MZM) which is driven by a bit pattern generation at a repetition rate of 10 Gb/s with a fixed pattern of one "1" per 32 bits. The erbium-doped fiber amplifier (EDFA) is used to compensate for the insert loss of the modulator. All the polarization controllers (PC1–PC4) are well adjusted. PC1 and PC2 are used to ensure the coherent combination of the CW light and the CCW light totally at OC4. Tuning PC3 and PC4, the polarization states of the pass port and the reflection port from the NOLM are made orthogonal, so these two beams are incoherently combined at the PBC. The position of the SOA in the loop can be adjusted by OTDL2 and the relative delay of the CW light and the CCW light is adjusted to be nearly 150 ps. The polarization beam coupler is used to incoherently combine the output signals of the pass port and reflection port of the NOLM and the relative delay of these two signals can be tuned by OTDL1. Two optical switches, SW1 and SW2, are used to control the connection of these two signals. The BPF1 with a fixed central wavelength of 1549.2 nm and a 3-dB bandwidth of 1 nm is used to filter out Probe 1. When SW1 is connected and SW2 is disconnected, the output of the BPF1 is two peaks as shown in Fig. 5(a). Conversely, when we connect the SW2 and disconnect SW1, the output of BPF1 is two notches as shown in Fig. 5(b). When both SW1 and SW2 are connected and the OTDL1 is tuned properly and the relative delay between the pass port and the reflection port of the NOLM is nearly 60 ps, the output of the BPF1 is a monocycle pair (+), as shown in Fig. 5(c). Then we change the OTDL2 so that the relative delay becomes −60 ps, the output waveform becomes a reversed monocycle pair (−) as shown in Fig. 5(d).

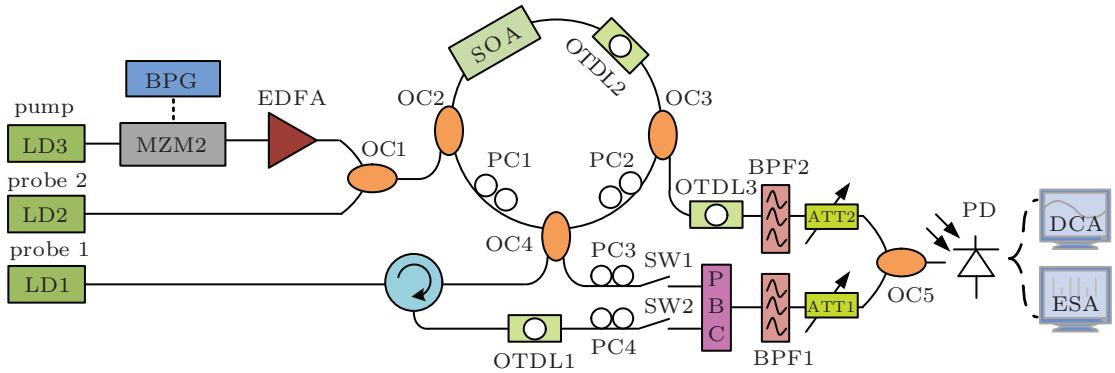


Fig. 4. (color online) Experimental setup for power-efficient UWB generation, ATT: attenuator, OC: optical coupler, ODL: optical delay line, BPG: bit pattern generator, EDFA: erbium-doped fiber amplifier, PD: photodetector. Experimental setup of photonic multi-shape UWB signal generation, LD: laser diode, MZM: Mach–Zehnder modulator, BPG: bit pattern generator, EDFA: erbium-doped fiber amplifier, ATT: attenuator, PC: polarization controller, SW: optical switcher, PD: photodetector.

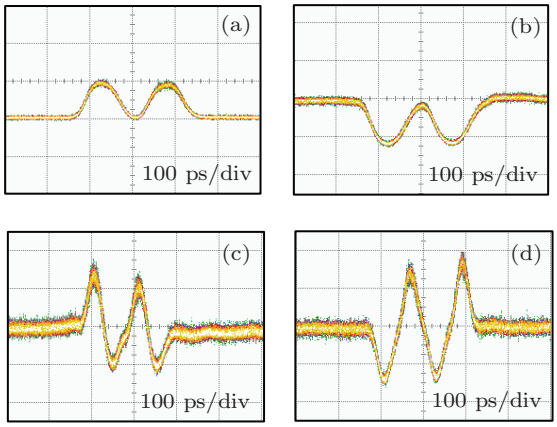


Fig. 5. (color online) Output waveforms of Probe 1 under different connection states of SW1 and SW2: (a) two peaks, (b) two notches, (c) monocycle pair (+), and (d) monocycle pair (−).

Now the output signals of BPF1 and BPF2 are coupled by OC5 and their relative delay is tuned by OTDL3. The weight of these two output waveforms can be tuned by two optical attenuators, ATT1 and ATT2, respectively. The final output waveform of the whole system is detected by a photodetector (PD). The temporal waveform and the radio frequency (RF) spectrum of the output signals are analyzed through a digital communications analyzer (DCA) and an electrical spectrum analyzer (ESA), respectively.

Initially, both SW1 and SW2 are disconnected. We carefully tune the BPF2 so that the probe carrier is located at the positive and negative linear slopes of the BPF2. Then a pair of polarity-reversed monocycle pulses is generated via phase modulation-to-intensity modulation conversion. The temporal waveforms and corresponding electrical spectra are shown in Fig. 6. One can see that the UWB pulse duration is about 200 ps. The UWB RF spectra have a relevant high energy in the low frequency region. In order to meet the FCC mask, the RF spectra in the low frequency region should be suppressed by using a low cut filter.

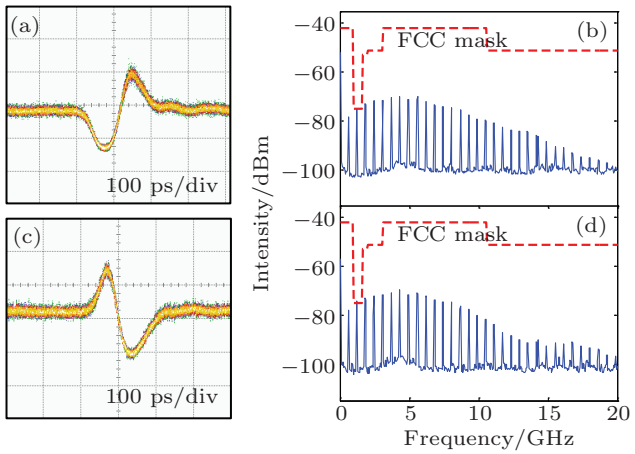


Fig. 6. (color online) Bi-polar monocycle pulses and their corresponding electrical spectra.

Now we connect SW1 and tune the central wavelength of BPF2 at 1554.8 nm, equal to the wavelength of Probe 2. Thus the output waveform of BPF2 is an intensity notch. After adjusting the OTDL2, OTDL3, ATT1, and ATT2 properly, a positive doublet pulse is generated at the output port of OC5 as shown in Fig. 7(a) and its corresponding RF spectrum is shown in Fig. 7(b). One can see the pulse width is 250 ps, and the 10-dB bandwidth of RF spectrum is about 6.6 GHz (from 2.6 GHz to 9.2 GHz). Then we disconnect SW1 but connect SW2 and retune the central wavelength of BPF2 at 1561.4nm, equal to the pump wavelength. Thus the output waveform of BPF2 is an intensity peak. As such, a negative doublet pulse is generated as shown in Fig. 7(c) and the measured RF spectrum is shown in Fig. 7(d). One can see the pulse width is 260 ps, and the 10-dB bandwidth of RF spectrum is about 6.2 GHz (from 2.4 GHz to 8.6 GHz). It should be noted that a doublet waveform can also be generated only by detuning BPF2. However the doublet shape cannot be adjusted freely. In our system, the doublet pulse is formed by one intensity peak and two intensity notches. The amplitudes of the peak and notches can be easily adjusted by ATT1 and ATT2. Thus the generated UWB waveform can be optimized. Furthermore, the duration of the generated doublet pulse becomes small as the probe delay of the peak and notches decrease. In terms of the frequency domain, the 10-dB bandwidth of the UWB pulse will be broader and the fraction bandwidth will be greater. Thus the electrical spectrum of this doublet pulse can be optimized and a more power-efficient spectrum can be achieved. From Figs. 7(b) and 7(d), one can see that the low frequency components are greatly suppressed compared to the RF spectra of monocycle pulses.

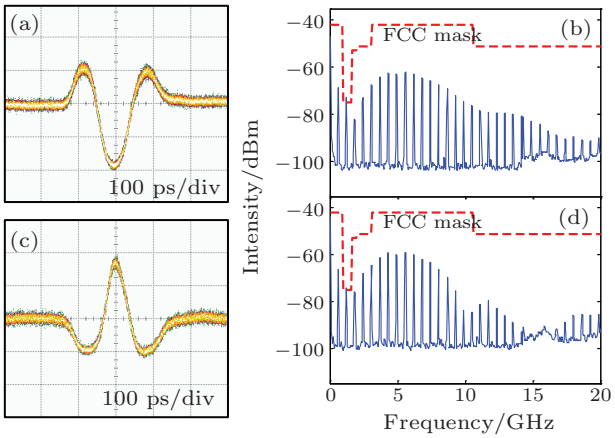


Fig. 7. (color online) Bi-polar doublet pulses and their corresponding electrical spectra.

Here we connect SW1 and SW2 simultaneously and tuning the OTDL1 properly, the output waveform of the BPF1 is the monocycle pair (+). Then we tune the central wavelength of BPF2 so that the output of the BPF2 is a negative monocycle pulse. After tuning the OTDL3, ATT1, and ATT2 properly, a positive triplet pulse is generated as shown in Fig. 8(a) and its corresponding electrical spectrum is shown in Fig. 8(b). One can see the pulse width is 220 ps, and the 10-dB bandwidth of RF spectrum is about 12.5 GHz (from 5.6 GHz to 18.1 GHz).

In order to obtain a polarity-reversed triplet pulse, we readjust the OTDL1, then the output waveform of BPF1 becomes the monocycle pair (−), as discussed in Fig. 3(a), and the output waveform of the BPF2 is changed to a positive monocycle pulse by tuning BPF2. Therefore the combined waveform becomes a polarity-reversed triplet pulse as shown in Fig. 8(c). The corresponding RF spectrum is shown in Fig. 8(d). One can see the pulse width is 230 ps, and the 10-dB bandwidth of the RF spectrum is about 8.6 GHz (from 5.6 GHz to 14.2 GHz).

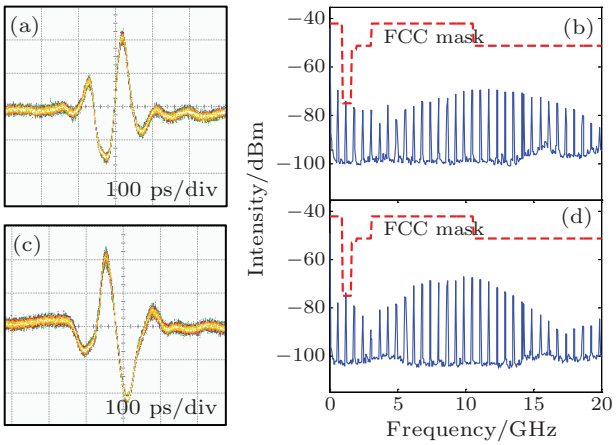


Fig. 8. (color online) Bi-polar triplet pulses and their corresponding electrical spectra.

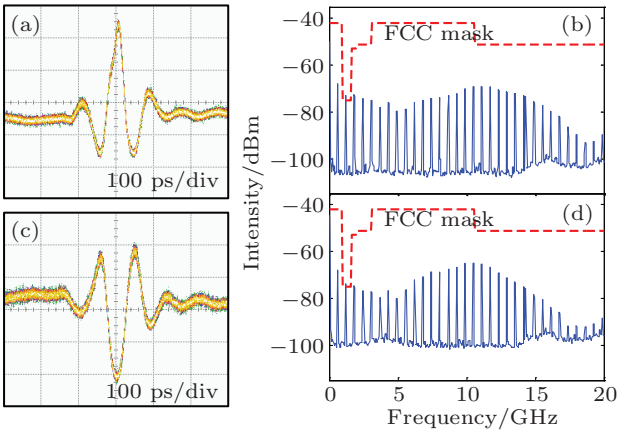


Fig. 9. (color online) Bi-polar quadruplet pulses and their corresponding electrical spectra.

As illustrated in Fig. 2(f), a quadruplet waveform can be generated by combining the peak pair and negative doublet pulse. Now we change the central wavelength of BPF2 properly to obtain a negative doublet pulse. Then the SW2 is disconnected and the OTDL3, ATT1, and ATT2 are properly adjusted, the output of the system is a quadruplet pulse as shown in Fig. 9(a) and its corresponding electrical spectrum is shown in Fig. 9(b). One can see the pulse width is 260 ps, and the 10-dB bandwidth of RF spectrum is about 10.6 GHz (from 5.5 GHz to 16.1 GHz). Similarly, we obtain a positive doublet pulse at the output of BPF2 by tuning the central wavelength of BPF2. Then we disconnect SW1 but connect SW2, a negative quadruplet pulse is generated as shown in Fig. 9(c) and its corresponding electrical spectrum is shown in Fig. 9(d). One can see the pulse width is 280 ps, and the 10-dB bandwidth of RF spectrum is about 8.1 GHz (from 6.1 GHz to 14.2 GHz). From the RF spectra of Fig. 8 and Fig. 9, we find the central frequency shifts to the high frequency, around 10 GHz. The reason for this lies in the fact that the pulse width of these high order UWB pulses is rather narrow. By optimizing the UWB pulse width, a better RF spectrum is achievable.

In our experiment, both bi-polar and multi-shape UWB pulses have been demonstrated. Thus the pulse polarity modulation (PPM) and pulse shape modulation (PSM) of UWB signals are feasible. Furthermore, the duration of the generated UWB pulses can be adjusted by the OTDLs in the system. In this way, the electrical spectra of the UWB pulses can be optimized and then power-efficient UWB pulses can be obtained. However, the high order UWB pulses are generated by summation of the multi-pulses with different wavelengths. So dispersion compensation technology should be adopted to increase the propagation distance of the UWB pulse. In addition, polarization controllers should be finely adjusted to increase the stability of the system.

4. Conclusion

In this paper, we have proposed and demonstrated the photonic generation of multi-shape UWB pulses using an SOA-based MOLM. When a Gaussian pulse is launched to the system, all monocycle, doublet, triplet, and quadruplet pulses are generated by combining the pump light and the probe light properly according to the specific rules described in Fig. 3. The shapes of the generated high-order UWB pulses are easily and flexibly adjusted and optimized. Thus the generated UWB pulses can be power-efficient.

References

[1] Aiello G R and Rogerson G D 2003 *IEEE Microwave Mag.* **4** 36
[2] Dong J J, Luo B W, Yu Y and Zhang X L 2012 *Chin. Phys.* B **21** 068401
[3] Ran M, Lembrikov B I and Ben Ezra Y 2010 *IEEE Photon. J.* **2** 36
[4] Yu Y, Dong J J, Li X and Zhang X L 2011 *IEEE Photon. Technol. Lett.* **23** 1754
[5] Dong J J, Zhang X L, Xu J, Fu S N, Shum P and Huang D X 2007 *Opt. Lett.* **32** 1223
[6] Yao J P, Zeng F and Wang Q 2007 *Opt. Lett.* **25** 3219
[7] Tan K, Shao J, Sun J Q and Wang J 2012 *Opt. Express* **20** 1184
[8] Dong J J, Yu Y, Zhang Y, Li X, Huang D X and Zhang X L 2011 *Opt. Express* **19** 10587
[9] Dong J J, Luo B W, Yu Y and Zhang X L 2012 *Chin. Phys.* B **21** 043201
[10] Dong J J and Huang D X 2007 *Opt. Lett.* **32** 2158
[11] Yu. Y, Dong J J, Li X and Zhang X L 2012 *IEEE Photon. J.* **4** 326
[12] Luo B W, Dong J J, Yu Y, Yang T and Zhang X L 2012 *Opt. Lett.* **37** 2217
[13] Huang T Y, Li J, Sun J Q and Chen L R 2011 *Opt. Express* **19** 15885
[14] Huang H, Xu K, Li J Q, Wu J, Hong X B and Lin J T 2008 *Opt. Lett.* **15** 2635
[15] Ou P, Zhang Y and Zhang C X 2008 *Opt. Express* **16** 5130
[16] Chen H W, Chen M H, Wang T L, Li M and Xie S Z 2008 *J. Lightwave Technol.* **26** 2492
[17] Zhang M J, Liu T G, Wang A B, Zheng J Y, Meng L N, Zhang Z X and Wang Y C 2011 *Opt. Lett.* **36** 1008
[18] Peled Y, Tur M and Zadok A 2010 *IEEE Photon. Technol. Lett.* **22** 1692